

## Supplementary Material

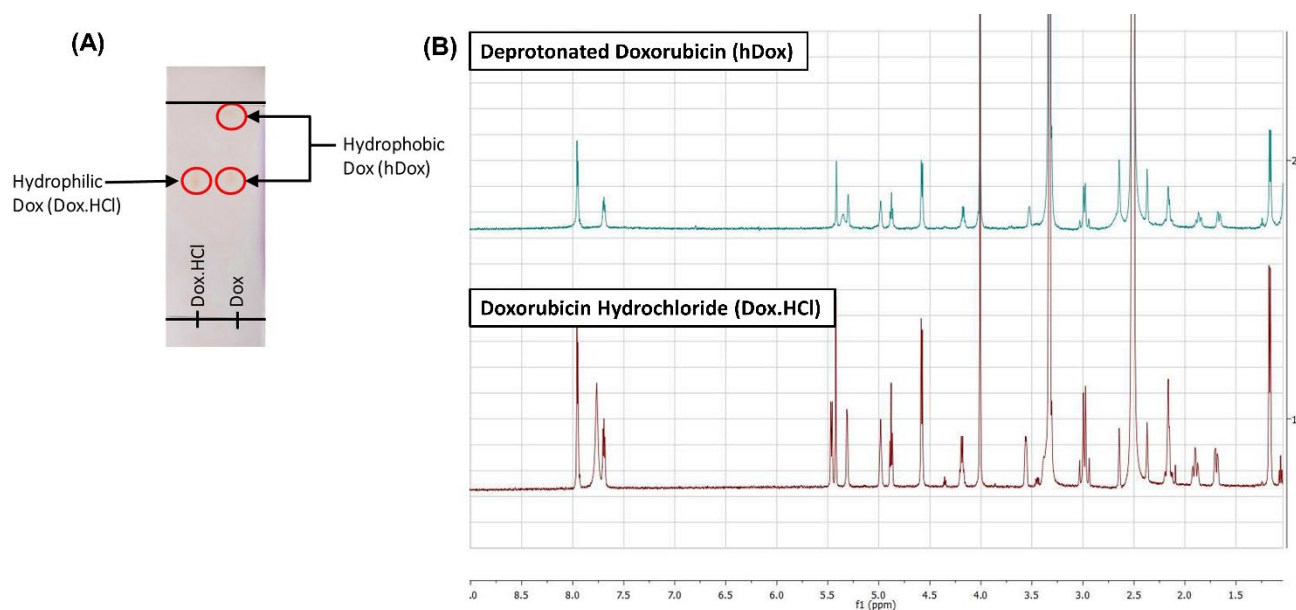
### *Increasing Doxorubicin Loading in Lipid-Shelled Perfluoropropane Nanobubbles via a Simple Deprotonation Strategy*

Pinunta Nittayacharn<sup>1</sup>, Eric Abenojar<sup>2</sup>, Al De Leon<sup>2</sup>, Dana Wegierak<sup>3</sup>, Agata A. Exner<sup>1,2\*</sup>

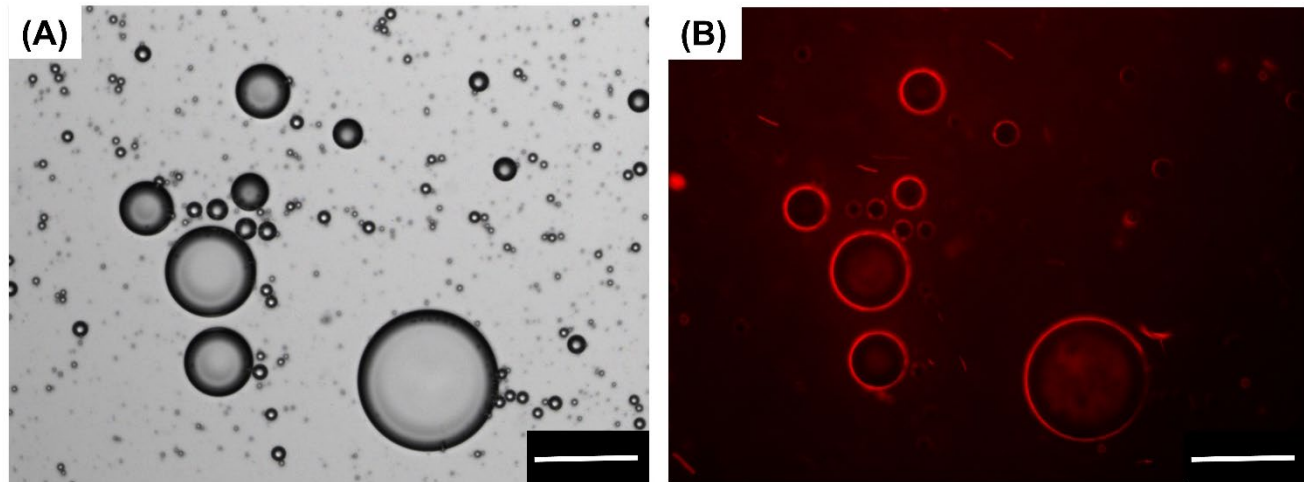
<sup>1</sup> Department of Biomedical Engineering, Case Western Reserve University, Cleveland, OH, USA

<sup>2</sup> Department of Radiology, Case Western Reserve University, Cleveland, OH, USA.

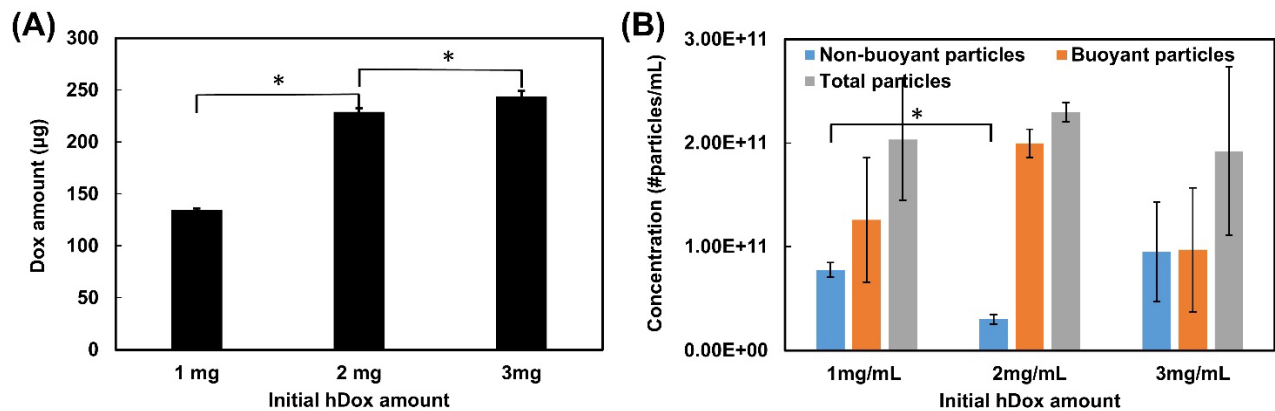
<sup>3</sup> Department of Physics, Ryerson University, Toronto, Canada.



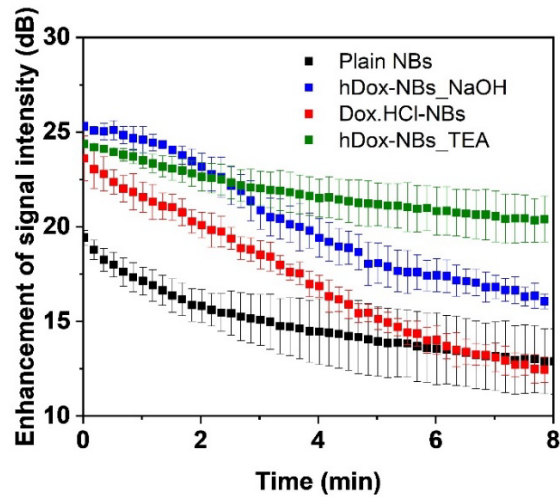
**Supplementary Figure 1.** (a) TLC plate showing the state of hydrophilic Dox (Dox.HCl, left lane) and hydrophobic Dox (hDox, right lane); (b) NMR spectrum showing the main structure of hDox and Dox.HCl. The analysis shows that the primary structure of Dox remains intact following the deprotonation process.



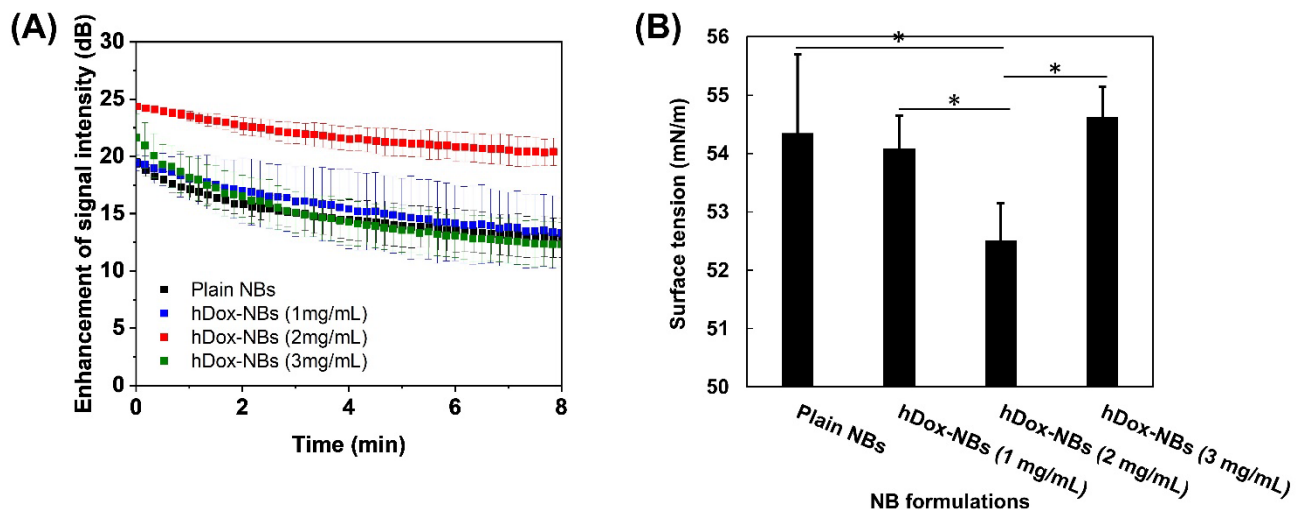
**Supplementary Figure 2.** Representative (a) bright field and (b) fluorescence image of hDox microbubbles showing co-localized hDox on the shell. The analysis was carried out on bubbles before isolation of nanobubbles to improve visualization of the bubble shell. Scale bar is 10  $\mu\text{m}$ .



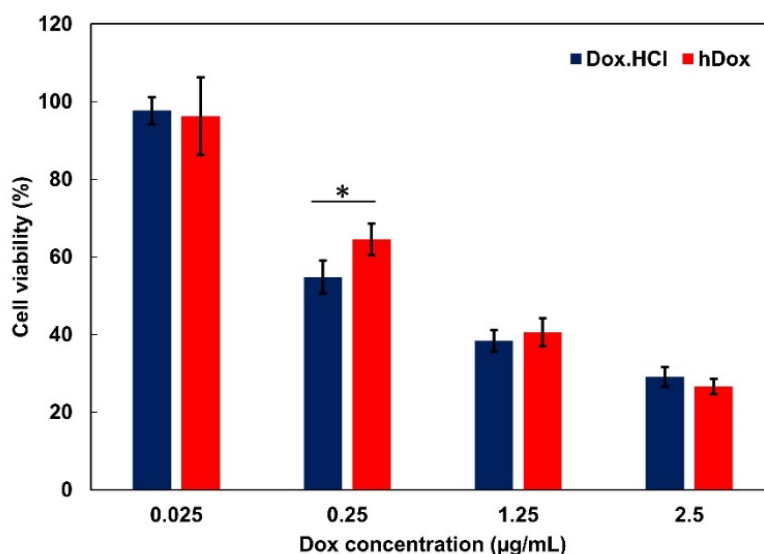
**Supplementary Figure 3.** Optimization of hDox-NB formulation ( $n=3$ ). (a) Total mass of hDox extracted from NBs following loading at various initial hDox feeding concentration used in the bubble preparation; (b) Concentration of buoyant and non-buoyant particles measured by RMM for each hDox loading amount. 2 mg/mL loading was selected from this optimization because it provided both a high hDox content in NBs and a consistently high yield of buoyant particles in the total particle population (as shown in (b)). Error bars represent standard deviation. Asterisk indicates  $p < 0.05$ .



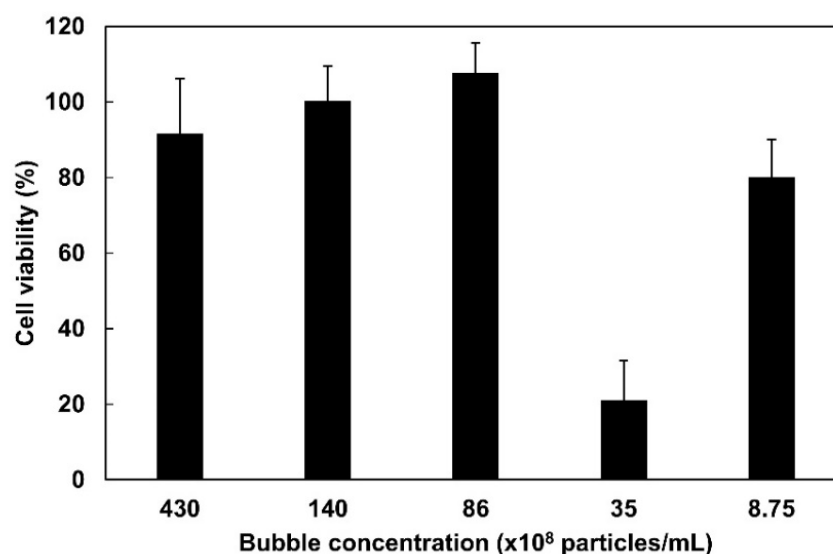
**Supplementary Figure 4.** Ultrasound signal decay of hDox-NBs (n=3) made from Dox that was deprotonated using either triethylamine or TEA (green squares) and NaOH (blue squares). The rate of decay of ultrasound signal from NBs made with TEA-deprotonated Dox was significantly slower than that of either plain NBs, Dox.HCl-NBs or NBs loaded with hDox deprotonated with NaOH. Error bars represent standard deviation.



**Supplementary Figure 5.** (a) Ultrasound signal decay of hDox-NBs (n=3) at various initial hDox concentration; (b) Surface tension measurements of NB formulations with increasing amounts of hDox. The measurements were acquired using a pendant drop tensiometer method and were repeated in triplicate. Error bars represent standard deviation. Asterisk indicates  $p < 0.05$ . The optimized NB formulation has slowest signal decay rate and the lowest surface tension.



**Supplementary Figure 6.** Cytotoxicity of doxorubicin hydrochloride (Dox.HCl) and hydrophobic deprotonated Dox (hDox) in OVCAR-3 cells evaluated 72h after treatment. Assays were carried out in triplicate. Error bars represent standard deviation. No difference was seen between the hDox and Dox.HCl treatment groups.



**Supplementary Figure S7.** Viability of OVCAR-3 cells following exposure to plain NBs and ultrasound at various NB concentrations. The WST-1 viability testing was performed 72h after treatment. All of the experiments were carried out in triplicate. Error bars represent standard deviation. Control plain NBs at 8.75 x10<sup>8</sup> particles/mL which is equivalent to the concentration of hDox-NBs used in cell viability experiments has cell viability at 80%.